Use of ^{1}H NMR Spectroscopy and Computer Simulations To Analyze Histidine pK_a Changes in a Protein Tyrosine Phosphatase: Experimental and Theoretical Determination of Electrostatic Properties in a Small Protein†

Patrick A. Tishmack,‡ Donald Bashford,§ Etti Harms,|| and Robert L. Van Etten*,‡

Department of Chemistry and Department of Biological Sciences, Purdue University, West Lafayette, Indiana 47907, and Department of Molecular Biology, The Scripps Research Institute, La Jolla, California 92037

Received May 27, 1997; Revised Manuscript Received July 23, 1997⊗

ABSTRACT: In bovine low M_r protein tyrosine phosphatase, the pK_a values of His-66 and His-72 are 8.3 and 9.2, respectively. These unusually high values were hypothesized to be caused by electrostatic interactions with several nearby negatively charged groups. To test this, mutant enzymes were made in which one or more carboxylate side chains were removed or introduced near the histidines. Michaelis kinetic parameters, measured using *p*-nitrophenyl phosphate as a substrate, indicated that all mutant enzymes retained approximately 50% or more of the activity of wild-type enzyme. The effect that each mutation had on the pK_a of the nearby histidine was monitored by ^{1}H NMR spectroscopy using the MLEV-17 pulse sequence to filter out the broad interfering amide resonances in the spectra. Independently, computer simulations of the pK_as were obtained using the finite difference method to solve the linear Poisson−Boltzmann equation. The proximity of a charged residue to the titrating histidine imidazole largely determined the extent of the pK_a perturbation. The change in pK_a for His-72 in the mutant enzymes was −1.69 units for D42A, −2.36 units for E23A, −2.99 units for E23A/D42A, and unchanged for E139A and Q143E. Thus, the pK_a of His-72 in the double mutant E23A/D42A decreased to nearly that of a free histidine imidazole group. The His-66 pK_a change was −1.25 units for E139A and was not significant for the other mutants. His-66, Glu-139, and Gln-143 are at the protein surface and much more exposed to the higher solvent dielectric compared to His-72, Glu-23, and Asp-42. These structural characteristics explain the smaller decrease in the observed pK_a of His-66 for the E139A mutant compared to the decrease in the pK_a of His-72 when a single nearby carboxylate was removed. These observations were adequately predicted by theoretical electrostatic calculations using the Poisson−Boltzmann equation as a model for a solute molecule of low dielectric in solution of high dielectric.

Bovine protein tyrosine phosphatase (BPTP)[1] is a low molecular weight cytoplasmic enzyme consisting of 157 amino acid residues with a total M_r of ∼18 000. This protein and the homologous human forms have been previously isolated from bovine (Lawrence & Van Etten, 1981; Zhang & Van Etten, 1990) or human (Waheed et al., 1988) tissue, and they have been cloned and overexpressed in *Escherichia coli* (Wo et al., 1992a,b). Similar phosphatases are also found in yeast and bacteria (Li & Strohl, 1996; Ostanin et al., 1995). The mammalian low M_r PTPs have 80−95% sequence identity and approximately 40% identity to yeast enzymes (Zhang et al., 1995). The enzymatic role of PTPs, removal of a phosphate group from a phosphotyrosine substrate, is essentially the reverse of protein tyrosine kinases. Tyrosine phosphatases are involved in cell cycle regulation, cell growth and differentiation, and signal transduction, and are important in balancing the phosphorylation reactions of protein tyrosine kinases (Yang & Tonks, 1993).

The known *in vitro* substrates for BPTP are aromatic phosphates and small peptidyl phosphates, as well as some acyl phosphates. BPTP catalyzes the dephosphorylation of the artificial substrate *p*NPP at pH 5.0 and 37 °C with a K_m of 0.3−0.4 mM and a V_{max} of 90−114 units/mg. It efficiently catalyzes the hydrolysis of phophotyrosyl residues of red cell band 3 and of autophosphorylated kinases (Waheed et al., 1988; Wo et al., 1992a; Zhang & Van Etten, 1990). EGF receptor, PDGF receptor, and insulin receptor are also dephosphorylated *in vitro* by BPTP (Ramponi, 1994; Shimohama et al., 1994). The actual cellular substrates for most low M_r PTPs are not known at this time.

The CXXXXXR sequence at the active site is common to all known PTPs including low and high M_r PTPs. In BPTP, the conserved residues at the ends of this sequence are Cys-12 and Arg-18, and the necessity of these two residues for catalysis is demonstrated by the complete loss of phosphatase activity when either amino acid is mutated

† This work was supported by U.S. Department of Health and Human Services Research Grant GM-27003 and by National Institutes of Health Grant GM45607.

* To whom correspondence should be addressed. FAX: 765-494-0239.

‡ Department of Chemistry, Purdue University.

§ The Scripps Research Institute.

|| Department of Biological Sciences, Purdue University.

⊗ Abstract published in *Advance ACS Abstracts,* September 15, 1997.

[1] Abbreviations: BPTP, bovine low M_r protein tyrosine phosphatase with the amino acid and cDNA sequences as described in Wo et al. (1992a); D_2O, deuterium oxide; DSS, 2,2-dimethyl-2-silapentane-5-sulfonate; EDTA, ethylenediaminetetraacetic acid disodium salt dihydrate; EGF, epidermal growth factor; HEPES, 4-(2-hydroxyethyl)-1-piperazineethanesulfonic acid; k_{cat}, catalytic rate constant or turnover number; K_m, Michaelis−Menten constant; MLEV-17, modified version of a decoupling pulse sequence from Levitt et al. (1982); NMR, nuclear magnetic resonance; PDGF, platelet-derived growth factor; *p*NPP, *p*-nitrophenyl phosphate; PTP, protein tyrosine phosphatase; SDS−PAGE, sodium dodecyl sulfate−polyacrylamide gel electrophoresis; V_{max}, enzyme velocity at saturating substrate concentration.

S0006-2960(97)01244-0 CCC: $14.00

to an alanine (Davis et al., 1994a,b). Although low M_r PTPs do not have the same conserved phosphate binding loop sequence, GXGXXG, found in many high M_r PTPs (Zhang & Dixon, 1994), a functionally similar phosphate binding loop is present at the active site (Zhang, M., et al., 1994; Evans et al., 1996).

The kinetic mechanism for catalysis by BPTP is well understood and serves as a paradigm for the structurally less extensively investigated high M_r PTPs. Cys-12 is the active site nucleophile in BPTP, backbone N−Hs as well as the side chain of Arg-18 are necessary for binding the phosphate group of the substrate and the transition state (Zhang et al., 1997), and Asp-129 acts as a critical proton donor for the leaving group (Davis et al., 1994a,b; Zhang, Z.-Y., et al., 1994). Hydrolysis of the phosphoenzyme intermediate is rate-limiting, at least in the hydrolysis reaction of activated substrates. The dephosphorylation proceeds with overall retention of configuration at phosphorus, and involves sequential S_N2 reactions with inversion in each step (Saini et al., 1981). A detailed structural model of a transition state analog complex has been described (Zhang et al., 1997).

The role of histidine residues in the catalytic process has been a subject of controversy. It was claimed that His-66 and His-72 in BPTP were located near the active site and participated in enzymatic catalysis (Chiarugi et al., 1994). In those studies, single mutants of each histidine (H66Q and H72Q) had sharply reduced activity, and the double mutant (H66,72Q) was apparently completely inactive. However, careful pH titration and kinetic studies on nonfusion BPTP proteins containing single and double histidine mutations together with the subsequent X-ray crystal and NMR solution structure determinations clearly demonstrated that His-72 and His-66 are approximately 9 and 18 Å away from the active site cysteine, and that neither histidine is directly involved in catalysis (Davis et al., 1994b; Logan et al., 1994; Zhang, M., et al., 1994; Su et al., 1994). Moreover, although BPTP is inactivated by treatment with diethyl pyrocarbonate, a double mutant containing no histidines whatsoever is kinetically active, and its activity is similarly lost upon treatment with diethyl pyrocarbonate (Davis et al., 1994b).

Although it plays no direct catalytic role, His-72 does play an important structural role, particularly by virtue of its interaction with Asn-15 (Zhang, M., et al., 1994; Evans et al., 1996). In this regard, the pK_a value of His-72, and to a lesser extent that of His-66, is of particular interest. These residues are unusually basic, with pK_a values of 8.4 and 9.2 for His-66 and His-72, respectively (Zhou et al., 1993). From the X-ray crystal structure of BPTP, His-72 is hydrogen-bonded to Asn-15 and is positioned 3.3 Å from Glu-23. Asp-42 is also in close proximity (4.3 Å) to His-72 while Glu-139 is near (3.6 Å) His-66. This suggested that acidic groups and hydrogen bonds could be largely responsible for the unusually high pK_a values observed for the histidines. Figure 1 shows the positioning of several important side chains relative to His-66 and His-72.

The measurement of pK_a changes of histidines and other residues in proteins has been done by kinetic methods (Russell et al., 1987), fluorescence titration (Loewenthal et al., 1993), and ^{1}H NMR spectroscopy (Loewenthal et al., 1992; Markley, 1975a; Sancho et al., 1992). Proton NMR spectroscopy is particularly convenient for observing the effects of electrostatic changes near the imidazole ring of histidine residues in proteins (Markley, 1975a). In BPTP, the two histidines are in substantially different environments, and the enzyme is also small enough to give relatively sharp resonance lines. The ^{1}H NMR chemical shifts of the C_2H and C_5H resonances during pH titrations are a direct means of determining histidine pK_as because the spectrum represents the average protonation state of the imidazole ring (Meadows, 1972). Because of the unique resonance positions and relatively sharp line widths, the imidazole C_2H and C_5H peaks of histidine were the first to be assigned unambiguously by ^{1}H NMR spectroscopy of proteins (Meadows et al., 1967). This technique was soon utilized by numerous researchers because it provided a means of directly examining the active site histidines of several enzymes in solution (Markley, 1975a). The NMR titration curves observed for histidines were useful in early studies of electrostatics because they provided empirical data with which to examine models of electrostatic theory for proteins (Botelho et al., 1978; Botelho & Gurd, 1978; Markley & Finkenstadt, 1975; Shire et al., 1974a,b).

The use of simplified electrostatic models in calculations of protein titration dates back to Linderstrøm-Lang (1924), who assumed the titrating charge to be spread uniformly over the surface of a sphere. Tanford and Kirkwood (1957) used symmetrically placed point charges to represent titrating sites inside a low dielectric sphere representing the protein environment, and analytical solutions of the linear Poisson−Boltzmann equation (eq 1) for the spherical geometry were used to obtain the electrostatic interactions between the sites.

$$\nabla[\epsilon(r)\nabla\phi(r)] - \kappa^2\epsilon(r)\phi(r) = -4\pi\rho(r) \qquad (1)$$

(The κ or Boltzmann term accounts for ionic strength effects.) As X-ray crystallographic structures of proteins became available, modified versions of the Tanford−Kirkwood procedure were introduced which incorporated some structural information but retained the basic spherical geometry (Matthew & Gurd, 1986). The rapid increase in available computing power made it possible to apply finite numerical methods to solve the Poisson−Boltzmann equation for dielectric geometries in which the details of the protein's atomic structure and solvent accessibility define a complex boundary between the interior low dielectric and the surrounding high dielectric solvent (Warwicker & Watson, 1982). This technology could then be applied to the protein titration problem where it allows not only for the calculation of site−site interactions, as in the Tanford−Kirkwood models, but also for interactions with nontitrating charges and dipoles and for the energetics of full or partial burial of titrating charges in the low dielectric environment (Bashford & Karplus, 1990). The treatment of the electrostatics of a solvent/solute system by a model in which the protein is a relatively low dielectric medium with embedded charges surrounded by a high dielectric solvent, and the boundary between dielectric regions is a complex one defined by the coordinates and radii of the atoms, is referred to here as Macroscopic Electrostatics with Atomic Detail, or MEAD. Models of this kind have been applied not only to protein titration but also to a variety of problems ranging from small molecule solvation to protein−DNA interactions (Honig & Nicholls, 1995; Gilson, 1995).

A major objective of the present study has been to understand some of the factors that cause unusually perturbed pK_a values of histidines. Therefore, the structural charac-

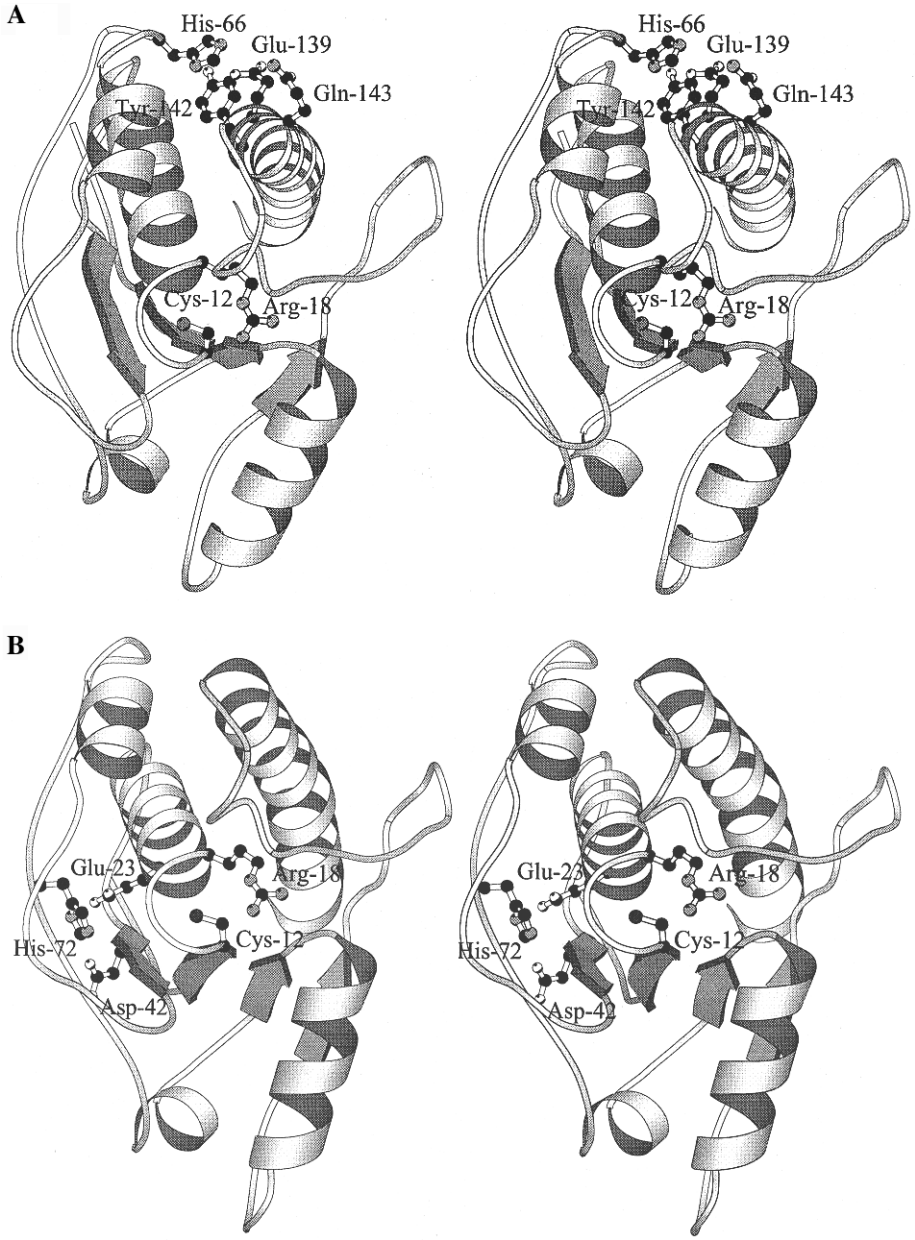

FIGURE 1: Stereoviews of wild-type BPTP made with MolScript (Kraulis, 1991) showing the important amino acid side chains (A) near His-66 and (B) near His-72 based on the published crystal structure (Zhang, M., et al., 1994, 1997). The solution structure of BPTP is known to be effectively identical (Logan et al., 1994).

teristics of BPTP which were important in producing these elevated pK_a values were examined by a series of single and double amino acid mutations. The measured changes in pK_a values for both His-66 and His-72 were then compared with theoretical electrostatic calculations. In view of the relative ease with which histidine pK_a values may be measured in proteins, they can serve very useful roles as reporter groups for studying electrostatic properties and for testing the validity of theoretical electrostatic predictions.

EXPERIMENTAL PROCEDURES

Materials. DSS (98%) and D_2O (99.9%) were obtained from Cambridge Isotopes Laboratories. DCl (99%) and NaOD (99%) were obtained from Aldrich. Standard solutions for pH calibration were from Fisher or Baxter. SP-Sephadex C-50 was obtained from Sigma, and Sephadex G-50 was from Pharmacia. The phosphatase substrate *p*-nitrophenyl phosphate was purchased from Sigma. All other materials were of the highest commercially available purity.

Mutagenesis. The cloning and expression of wild-type BPTP was described earlier (Wo et al., 1992a). For mutagenesis, a 765 base pair *Xba*I−*Bam*HI fragment containing the BPTP gene was transferred into the corresponding sites of bacteriophage M13mp18. The resulting single-stranded DNA was used as a template for mutagenesis (Vandeyar et al., 1988). The following primers were used to initiate second strand synthesis: (E23A) 5′-CATCG-CAGCTTGCGGTTTTC-3′, (D42A) 5′-GGGTCATTG-CAAGTGGCG-3′, (E139A) 5′-CCGACTTTGCTACCGTC-TACC-3′, and (Q143E) 5′-GAGACCGTCTACGAACA-GTGCGTG-3′. The changed bases are underlined. The codons GAA and GAG were changed to GCT to convert Glu-23 and Glu-139 to Ala, GAC was changed to GCA to convert Asp-42 to Ala, and CAG was changed to GAA to obtain Glu-143 in place of Gln. The primers were obtained

from the Purdue Macromolecular Synthesis Laboratory or, in the case of the Q143E primer, from Integrated DNA Technologies (Coralville, IA). Mutagenesis was performed using the T7 *in vitro* mutagenesis kit from U. S. Biochemical Co. An initial screening for the desired mutations was performed using single-lane nucleotide sequence reactions ("A-tracking") for the mutants D42A, E139A, and Q143E. The base changes that were introduced to make the E23A mutant created the recognition sequence for the restriction enzyme *Pvu*II which was utilized in screening for that mutant. The double mutant E23A/D42A was made by starting with the single-stranded DNA of the M13mp18 derivative that already contained the confirmed D42A mutation as the template. The same E23A primer noted above was then used to initiate second strand synthesis. Screening for the desired second mutation was done by confirming the introduction of an additional *Pvu*II restriction site. The resulting mutant BPTP *Xba*I−*Bam*HI fragments were excised from the bacteriophage M13mp18 derivatives and inserted into the analogous sites of the bacterial expression vector pET11d (Novagen Inc., Madison, WI) and subsequently transformed into the *Escherichia coli* strain BL21(DE3) for overexpression of the mutant BPTP proteins. The complete nucleotide sequences of the mutant BPTP genes in the final plasmid constructs were determined in order to verify the mutation as well as the integrity of the remainder of the gene.

Expression and Purification. All the enzymes were obtained by overexpression in *Escherichia coli* BL21(DE3) containing the appropriate plasmid. Approximately 50 mg of protein was obtained per liter of rich medium. The enzymes were purified by SP-Sephadex C-50 cation exchange followed by Sephadex G-50 size exclusion chromatography. Purity was assessed by discontinuous SDS−PAGE with 4% stacking gels and 12.5% resolving gels. Pure fractions containing 0.5−1.5 mg/mL protein were concentrated to make samples for NMR analysis.

Steady-State Kinetics. Kinetic parameters were obtained for each purified enzyme in 100 mM NaOAc, 85.5 mM NaCl, and 1 mM EDTA, 37 °C, pH 5.0, with 0.1−2.0 mM *p*NPP as substrate. The protein concentrations were 0.17−0.22 μM for all enzymes. Protein concentrations were determined by UV absorbance measurements at 280 nm using extinction coefficients previously measured at this wavelength (Davis et al., 1994a). The K_m and V_{max} were calculated by using a nonlinear least-squares fit of the data to the Michaelis−Menten equation.

^{1}H NMR Spectroscopy. Purified protein fractions were concentrated to ∼18−24 mg/mL (∼1.5−2.2 mM) in D_2O solution containing 130 mM NaCl and 20 mM NaH_2PO_4 usually 1−2 h before obtaining spectra. The enzyme for each sample was concentrated to <0.5 mL in a Filtron 10 mL Omegacell disposable stirred cell ultrafiltration device with a 3 kDa nominal molecular mass cutoff membrane filter. The solution was reconstituted with 1 mL of D_2O and concentrated again. This procedure was repeated once with D_2O and then 3 times with the salt and buffer solution in D_2O. Most of the residual water was removed in this manner. If further exchange of the amide protons for deuterons was desired, the sample was stored in a sealed tube at 4 °C for 12−16 h or longer. Proton NMR spectroscopy was performed on a Varian Unity Plus 600 spectrometer operating at 14.1 T (600 MHz for ^{1}H). All spectra were obtained at 25 ± 1 °C using Wilmad 528-PP 5 × 180 mm NMR tubes. The residual HOD resonance was referenced to 4.77 ppm versus an external DSS standard in D_2O at 25 °C. The standard ^{1}H NMR spectra were obtained with a 7200 Hz spectral width, 2 s acquisition time, 2 s relaxation delay, and 64 acquisitions, and processed with 64 000 points and a 0.4 s Gaussian apodization function. All MLEV-17 spectra were obtained with a 20 ms spin lock time, 7200 Hz spectral width, 1 s acquisition time, 1 s relaxation delay, and 128 acquisitions, and processed with 32 000 points and a 0.2 s Gaussian apodization function. The residual HOD resonance in all spectra was suppressed with a 20−30 Hz radio-frequency field during the relaxation delay and with the Varian solvent suppression algorithm to remove low-frequency signals.

pK_a Determination. The pH titrations were performed in at least 12 steps over the pH range 5−10.5. A Corning Digital 112 pH meter and an Ingold semimicro combination pH electrode were used to measure the pH before and after acquiring the NMR spectrum at each point. Because the glass electrode errors and pK_a shifts in D_2O solutions were constant and largely offsetting, no correction was made for the deuterium isotope effect (Glasoe & Long, 1960; Li et al., 1961; Roberts et al., 1969). The protein solution was titrated in a 2 mL Eppendorf tube and stirred with a small Teflon-coated stir bar. The pH was adjusted by gradually adding 2−5 μL aliquots of 0.1 M DCl or NaOD solutions with a narrow-diameter (0.6 mm OD) pipet tip. The pK_a values were obtained by fitting the NMR titration data to the modified Henderson−Hasselbalch equation (eq 2) or the modified Hill equation (eq 3) (Markley, 1975a; Markley & Finkenstadt, 1975) using the Marquardt−Levenberg nonlinear least-squares algorithm (SigmaPlot, Jandel Scientific).

$$\delta_{obs} = \delta_A + (\delta_{AH} - \delta_A) \times (10^{-pK_a})/(10^{-pK_a} + 10^{-pH}) \quad (2)$$

$$\delta_{obs} = \delta_A + (\delta_{AH} - \delta_A) \times (10^{-pK_a/n})/(10^{-pK_a/n} + 10^{-pH/n}) \quad (3)$$

For these equations, δ_{obs} is the observed chemical shift, δ_A is the chemical shift of the unprotonated imidazole, δ_{AH} is the chemical shift of the fully protonated imidazole, and n is the Hill coefficient. Proton chemical shifts can usually be measured to an accuracy of ±0.01−0.05 ppm (determined largely by the line width at half-maximum peak height) while the pH is generally no more accurate than approximately ±0.05 unit (Meadows, 1972). The measured pH typically also has an intrinsic error of 0.02 pH unit per millivolt change in liquid junction potential (Ramette, 1981). For this study, the precision for pH measurements varied from ±0.03 unit in the lower pH range (∼5−8) up to ±0.10 unit at higher pH (>8).

Theoretical pK_a Calculations. The general methods used for calculating pK_a values have been described in detail previously (Bashford & Gerwert, 1992) and will only be summarized here. It is assumed that the difference between the titration behavior of an ionizable group in the protein and that of the same group in a model compound can be accounted for by differences in the two electrostatic environments, and that these electrostatic environments can be represented by a MEAD model of the kind described in the introduction. One must therefore calculate the difference

in the electrostatic work of changing the charges from the protonated to the unprotonated state in the protein and in the model compound. Three kinds of energetic terms occur in the calculation: ΔG_{Born}, the interaction of the titrating charges with the polarization that these charges themselves induce in the surroundings (as in the Born solvation energy); ΔG_{back}, the interaction of the titrating charges with the background of nontitrating charges of the protein or model compound; and a matrix of interactions between titrating sites. For each titrating site in the protein, numerical solutions of the Poisson−Boltzmann equation (eq 1) corresponding to the protonated and deprotonated states of the site in the protein and the protonated and deprotonated states of the model compound must be obtained for the calculation of these energetic terms [see Bashford and Gerwert (1992) for details]. It is convenient to define an intermediate quantity, the intrinsic pK_a, or pK_{int}, which is the pK_a that an ionizable site in the protein would have if all other ionizable sites were held in their electrically neutral states. This quantity is independent of pH, and in the current context, it is calculated by the modification of the model compound pK_a by the Born and background terms:

$$pK_{int} = pK_{mod} - (2.303k_BT)^{-1}(\Delta G_{Born} + \Delta G_{back}) \quad (4)$$

Having obtained the pK_{int} values of each site, and the matrix of site−site interactions, one can, in principle, obtain the titration curve of each site by a Boltzmann-weighted sum over the 2^N possible protonation states of the protein, where N is the number of sites. In practice, this is not feasible for more than 15−20 sites, so the Monte-Carlo method of Beroza et al. (1991) has been used to obtain the curves. The reported pK_a values are the midpoints of these curves. For the two histidine residues in BPTP, we have included tautomerism by a pseudosite method described previously (Bashford et al., 1993).

Heavy-atom coordinates for wild-type BPTP are taken from the 1.9 Å resolution X-ray crystallographic structure of Zhang et al. (1997). The X-ray structure (Brookhaven PDB file 2PNT) contains a HEPES buffer molecule with its sulfonate group in the presumed position of the substrate phosphate group. The HEPES was removed, and a methyl phosphate molecule was modeled in its place. Water molecules were also deleted from the crystal structure. Further processing of the structures for the electrostatic calculations was done using the CHARMM molecular mechanics package which implements several empirical potential energy functions (Brooks et al., 1983). Two different wild-type structures were built: one using the CHARMM-19 parameter model in which polar hydrogen atoms are included explicitly but other hydrogens are merged into extended atoms (Reiher, 1985); and the other based on the CHARMM-22 model for proteins and lipids in which all hydrogen atoms are explicit (MacKerell et al., 1992; MacKerell and Karplus, unpublished results). Hydrogen atom positions for the fully protonated molecule were generated using the HBUILD facility (Brünger & Karplus, 1988) of CHARMM, supplemented by trial 180° rotations of the carboxylic acid groups of the Asp and Glu side chains and 120° rotations about the CH_3O-P bond of methyl phosphate to choose the protonation site resulting in the lowest energy. Because interactions with the Ser-19 hydroxyl group and other hydrogen bonding interactions are believed to help stabilize the negatively charged state of Cys-12, the active site nucleophile, an initial run of HBUILD was done with Cys-12 deprotonated; then Cys-12 was protonated and a second HBUILD run was done to place its proton. The CHARMM-22 structure was subjected to a two-step energy minimization protocol (You & Bashford, 1995) consisting of steepest descent minimization with no electrostatic terms, and a conjugate gradient minimization in which the dielectric constant of the electrostatic term is set to 4.0. The rms deviation of the minimized coordinates from those prior to minimization was 0.67 Å for all atoms and 0.47 Å for backbone atoms. No minimizations were performed for the CHARMM-19 structure. Mutation of Glu or Asp side chains to Ala was modeled by truncation of side chain atoms beyond the β-carbon from the relevant residue in the wild-type structures.

The electrostatic calculations were done using the multiflex program from the MEAD programming suite (Bashford & Gerwert, 1992). The groups treated as titrating sites in the calculation included methyl phosphate in the active site, the C- and N-termini of the protein, and all ionizable side chains except for those of Tyr, Lys, and Arg residues which were treated as fixed and protonated. The charges and Born radii used were taken from the partial charges and van der Waals minima of either the CHARMM-22 or the CHARMM-19 parameter sets, except that hydrogen atoms whose van der Waals minimum radii are less than 1.2 Å are assigned a radius of 1.2 Å. As in previous work (Bashford & Gerwert, 1992; Bashford et al., 1993), the full set of partial charges were used to describe the titrating sites rather than concentrating the entire formal charge on a single point. [The use of such charge models on titrating groups was recently found to give improved accuracy over the single-point method in calculations with low interior dielectric constants (Antosiewicz et al., 1996).] The model compounds for each site were the *N*-formyl-*N*-methylamide derivatives of the amino acids, and their coordinates were taken from the corresponding residues in the crystal structure along with their flanking peptide groups. The pK_{mod} values used were as given by Bashford et al. (1993) with the addition of 9.5 for Cys and 6.8 for methyl phosphate. The dielectric constant of the protein interior was set to 4.0, and the exterior was assigned a dielectric constant of 80 and an ionic strength of 0.15 M. A 2.0 Å counterion exclusion radius and a 1.4 Å solvent probe radius were used. The Poisson−Boltzmann equation for each site was solved by a finite-difference method using an initial coarse lattice having 81^3 nodes and 1.0 Å spacing centered on the protein, followed by a fine lattice with a 0.25 Å lattice spacing centered on the titrating sites.

RESULTS

The kinetic and spectroscopic evidence indicated that the structures of all the mutant proteins were very similar to that of wild type protein. The kinetic results for the BPTP enzymes are summarized in Table 1. The steady-state kinetic properties of the mutants did not differ greatly from wild-type BPTP, indicating that no detrimental structural or functional changes were produced. The apparent affinity for *p*NPP substrate was somewhat reduced for D42A and E23A/D42A (69% and 46% of wild-type BPTP, respectively). Interestingly, the catalytic rate of D42A was ~80% greater than that of wild type.

Table 1: Kinetic Constants of Wild-Type BPTP and BPTP Mutants[a]

enzyme	K_m (mM)	V_{max} (units/mg)	k_{cat} (s^{-1})	$k_{cat}/K_m \times 10^4$ (s^{-1} M^{-1})
WT	0.31 ± 0.01	92.0 ± 0.8	27.61 ± 0.3	8.99 ± 0.2
E23A	0.18 ± 0.01	59.6 ± 0.8	17.88 ± 0.2	9.93 ± 0.5
D42A	0.80 ± 0.04	166 ± 4	49.92 ± 1.2	6.23 ± 0.3
E23A/D42A	0.41 ± 0.02	57.4 ± 1.2	17.21 ± 0.4	4.18 ± 0.2
E139A	0.30 ± 0.01	109 ± 1.0	32.68 ± 0.3	10.9 ± 0.3
Q143E	0.34 ± 0.01	101 ± 1.5	30.23 ± 0.4	8.96 ± 0.4

[a] See Experimental Procedures for conditions. Standard errors are reported for all values.

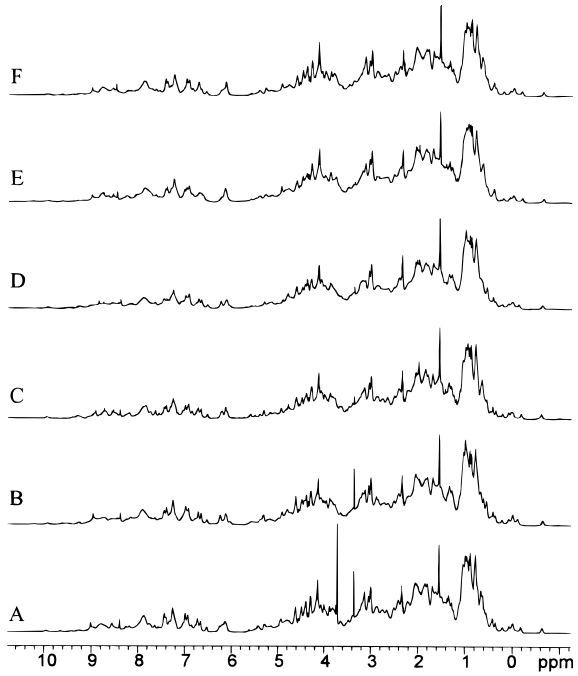

FIGURE 2: Conventional 1D ^{1}H NMR spectra of (A) wild-type BPTP, pH 4.93, (B) E23A, pH 4.88, (C) D42A, pH 4.75, (D) E23A/D42A, pH 4.60, (E) E139A, pH 4.71, and (F) Q143E, pH 4.98. The other conditions are as described under Experimental Procedures. The spectra are very similar throughout the entire frequency range, indicating that few structural differences exist. The sharp peaks at 3.4 and 3.8 ppm in some of the spectra are due to small amounts of low molecular weight impurities.

The mutant enzymes appeared to have secondary structures that were highly similar to wild-type BPTP (Logan et al., 1994), because their ^{1}H NMR spectra had the same overall chemical shift dispersion and peak pattern (Figure 2). The imidazole C_2 protons of both histidines were distinguished by their relatively narrow line widths compared to the amide protons and by their higher resonance frequencies compared with most other protons bonded to carbon. These properties were exploited for the pH titration experiments (*vide infra*). The chemical shifts of the C_2 protons generally varied from 8.3 ppm at pH ~5 to 7.4 ppm at pH ~10 for His-66 and approximately 9−8 ppm for His-72 over the same pH range. For the C_5 protons, the change in chemical shift was only 0.5 ppm or less for those that could be measured accurately.

The C_2H line widths observed for His-66 were 4−11 Hz while those of His-72 were 4−30 Hz over the pH range used in this study. Line broadening was much more apparent for His-72 than for His-66. The imidazole C_2 protons are expected to exchange more slowly than most of the protein backbone amide protons which resonate in the same frequency range (about 7.5−9.5 ppm). The slowly exchanging amide resonances overlap with the imidazole C_2 proton resonances and may obscure them during a titration, particularly because the C_2 proton peaks tend to broaden and lose intensity as the pH approaches the imidazole pK_a (Sudmeier et al., 1980). The rate of tautomerization of the imidazole N−H protons may also contribute to the observed C_2H line width because it falls into the intermediate exchange time scale where maximum broadening occurs. The proton exchange rates in proteins can be affected when using different buffers by either changing the on and off rates for protonation or causing slight conformational changes in the protein (Markley, 1975b,c; Sudmeier et al., 1980). A discontinuous titration curve may be obtained if intermediate exchange rate conditions exist for the imidazole group. This was noticed to some extent for the His-72 imidazole in all the enzymes in this study, and addition of phosphate buffer substantially improved the results for most cases. Phosphate buffer rather than acetate buffer was used for all the titrations because its pK_a is higher in the middle of the titration range than acetate (7.21 *vs* 4.75, respectively), and it is also a weak competitive inhibitor of BPTP which may help stabilize the enzyme during the titration. Although the ionic strength for phosphate buffer increases as pH is increased, this did not appear to be a problem because the pK_a values measured for His-66 and His-72 were essentially identical with and without phosphate present.

Exchange of amide protons for deuterons is a common method for decreasing the number of these broad resonances in ^{1}H NMR spectra. The extent of exchange is often forced by employing relatively high pH and temperature (pH 8−10 and 40−80 °C). However, the deuterium exchange conditions used for all the enzymes in the present study were very mild to prevent protein denaturation before or during the NMR experiments. Instead, a spectral editing pulse sequence was used to reduce the intensity of the amide proton resonances overlapping the histidine peaks in the ^{1}H NMR spectra of each enzyme (Davis et al., 1994b; Zhou et al., 1993). The MLEV-17 pulse train in these NMR experiments has the advantage of giving a better signal to noise ratio in the spectrum than earlier pulse sequences. A one-dimensional MLEV-17 experiment produces a spectrum where the observed signal intensity depends on the relaxation time of the proton and the length of time that the spin-lock is applied. Therefore, by setting the spin-lock time appropriately, amide proton resonances can be nearly eliminated while imidazole C_2 and C_5 protons and aromatic resonances are still observable in the higher frequency region of the spectrum.

Figure 3 shows a series of MLEV-17 ^{1}H NMR spectra for the titration experiments with wild-type BPTP and the E23A mutant. Differentiating between the His-66 and His-72 C_2H resonances in the E23A spectra appears to be difficult near pH 8, but a full inspection of their line shapes (including intermediate points not shown in Figure 3) and a nonlinear least-squares fit of the data to the theoretical titration curve

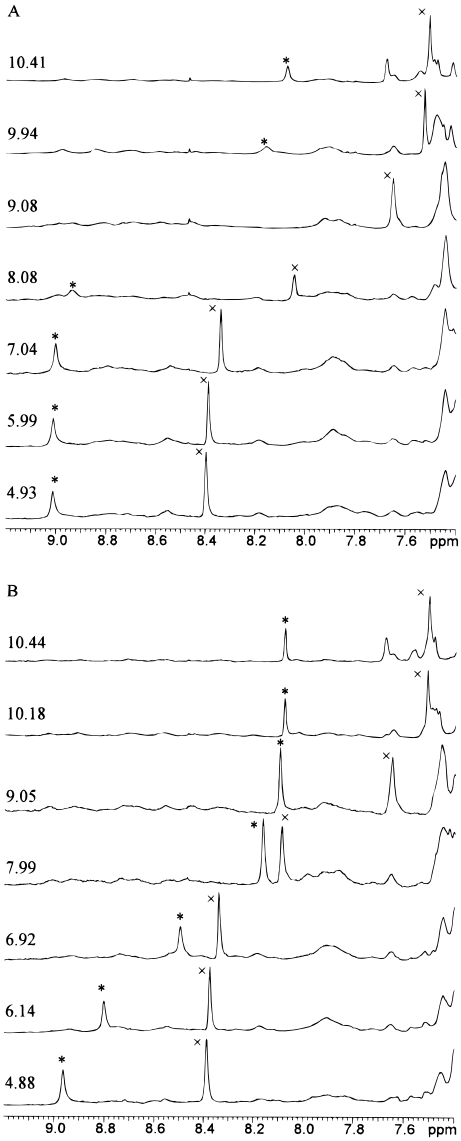

FIGURE 3: MLEV-17 ^{1}H NMR spectra of (A) wild-type BPTP and (B) E23A pH titrations with conditions as described under Experimental Procedures. The pH is shown above the corresponding spectrum for both titrations. The His-66 C_2H resonance is indicated by (×), and the His-72 C_2H resonance is indicated by (*). At pH 9.08 for wild type BPTP, the His-72 peak was too broad to observe.

clearly showed that the correct assignments were as labeled in Figure 3. The His-72 resonance for wild-type BPTP broadened substantially from pH 8 to 10. This was also noticed for the E139A and Q143E mutants but was much less in the other mutants. The line broadening of the C_2H resonance did not adversely affect the interpretation of the pH titration spectra.

Figure 4 shows two graphs of the pH titration data obtained for the C_2 and C_5 protons of the His-66 and His-72 imidazole groups in wild-type BPTP and the five mutants. Table 2 summarizes the pK_a values obtained from the pH titrations for the wild-type and mutant forms of BPTP. Hill coefficients were also calculated for each pK_a. A Hill coefficient that is significantly different from 1.0 indicates that multiple dissociating groups may be involved in the titration (Markley, 1973, 1975a; Markley & Finkenstadt, 1975). The pK_as of Q143E and the His-72 pK_a of E23A each had Hill coefficients that were statistically different from unity, but the deviations were small. The wild-type pK_a values of 8.29

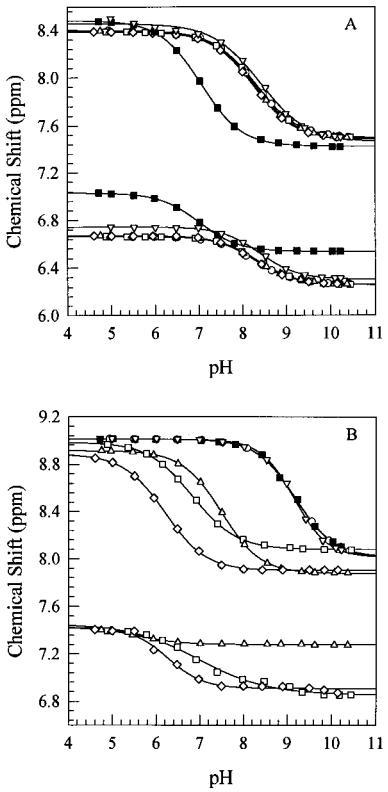

FIGURE 4: Graphs of the pH titration curves of (A) His-66 and (B) His-72 side chains based on the C_2H and C_5H chemical shifts for wild-type BPTP (○), E23A (□), D42A (△), E23A/D42A (◇), E139A (■), and Q143E (▽). The C_2H titrations are on the top portion of each graph, and the C_5H titrations are below them. The solid lines are nonlinear least-squares fits of the data to the modified Hill equation (eq 3). Graph A shows that both the C_2H and C_5H pH titrations of His-66 can be observed for all the proteins, and only the E139A and Q143E curves are not superimposable with the others. Graph B shows that only the three mutations affecting His-72 had observable C_5H titration points. The leftward shift of the His-72 titration curves is readily apparent.

for His-66 and 9.19 for His-72 are in excellent agreement with the values, 8.36 and 9.19, respectively, previously measured (Zhou et al., 1993). It is clear that the nearby carboxylate functions significantly affected the pK_as of each histidine, because the pK_a of His-66 or of His-72 was decreased only when a nearby carboxylate group was eliminated. The other histidine, located farther from the mutation site, was not affected. The greatest effect on the pK_a of His-72 was seen in the case of the double mutant E23A/D42A which decreased nearly 3 pK_a units compared to wild-type BPTP. The respective single mutants had intermediate effects on the pK_a of His-72. The E139A mutant caused a significant decrease in the pK_a of nearby His-66 but had no effect on the pK_a of the more distant His-72. The Q143E mutant, which introduced a negatively charged carboxylate near His-66, had only a minor effect on the pK_a.

The calculated pK_a values for His-72 and His-66 are summarized in Table 3. In all cases, the calculation placed the deprotonated form of His-72 in the ϵ tautomer and His-66 in the δ tautomer. As in the experimental measurements, unusually high pK_a values were found for both histidines in the wild-type protein, and the mutation of nearby glutamate or aspartate residues to alanine significantly lowered the pK_a values of the adjacent histidine but had little effect on the

Table 2: pH Titration of Histidine Residues in BPTP and BPTP Mutants[a]

enzyme	His-66 pK_a	His-66 ΔpK_a *vs* WT	His-72 pK_a	His-72 ΔpK_a *vs* WT
WT	8.29 ± 0.01	−	9.19 ± 0.01	−
E23A	8.32 ± 0.01	+0.03	6.83 ± 0.01	−2.36
D42A	8.26 ± 0.002	−0.03	7.50 ± 0.01	−1.69
E23A/D42A	8.25 ± 0.01	−0.04	6.20 ± 0.01	−2.99
E139A	7.05 ± 0.01	−1.24	9.18 ± 0.03	−0.01
Q143E	8.40 ± 0.04	+0.11	9.15 ± 0.02	−0.04

[a] See Experimental Procedures for conditions. Standard errors are reported for all values.

Table 3: Theoretical Calculations of pK_a Values[a]

			His-66	His-72
pK_a	WT	C22	9.04	11.36
		C19	7.49	10.18
		exp	8.29	9.19
ΔpK_a	E23A	C22	−0.07	−6.80
		C19	−0.05	−5.07
		exp	0.03	−2.36
	D42A	C22	0.01	−1.86
		C19	0.01	−1.57
		exp	−0.03	−1.69
	E23A/D42A	C22	−0.08	−7.93
		C19	−0.06	−5.11
		exp	−0.04	−2.99
	E139A	C22	−3.33	−0.07
		C19	−3.48	−0.06
		exp	−1.24	−0.01

[a] C22, C19, and exp denote calculations from the CHARMM-22 model, calculations from the CHARMM-19 model, and experimental results from Table 2, respectively. ΔpK_a values for mutants are relative to the wild type (WT). In all cases, the calculation placed the deprotonated form of His-72 in the ϵ tautomer and that of His-66 in the δ tautomer.

farther histidine. In many cases, the calculations overestimated the magnitude of the effects. Thus, the His-72 pK_a was too high for wild-type BPTP, and the magnitudes of the pK_a shifts for E23A, E23A/D42A, and E139A were significantly overestimated, although the shift for D42A was in good agreement with experiment. The overestimates were larger with the CHARMM-22 model than with the CHARMM-19 model.

The calculations also included methyl phosphate, the chain termini, and all Asp, Glu, and Cys side chains to account for the possibility that the pH dependence of the charges of these other groups affected the histidine titrations. If such pH dependence was neglected by fixing all Glu and Asp side chains and the methyl phosphate in the deprotonated state, and all Cys side chains in the protonated state, then the pK_a of His-72 in the wild-type protein was calculated to be 9.54 for the CHARMM-19 model and 11.51 for the CHARMM-22 model. These values differed from the corresponding calculated pK_a values of Table 3 by −0.64 and +0.13, respectively. The differences were caused by interactions of His-72 with Asp-129 (in the CHARMM-22 case) and the methyl phosphate and Cys-12 (in the CHARMM-19 case). Such effects were less than 0.3 pK unit in magnitude for His-66 in the wild type. In the mutant structures where the histidine pK_a values were in the neutral to acid range, the pH dependence of other carboxylate groups can have significant and complex effects. The nonadditivity of the ΔpK_a values for the E23A and D42A mutants and the double mutant (also seen experimentally, although to a lesser degree) was a result of this pH dependence.

DISCUSSION

The pK_a of an imidazole group is approximately 6.1 for a free histidine in aqueous solution, but the structural characteristics of wild-type BPTP significantly increase the pK_a values of both His-66 and His-72. The proximity of carboxylate groups to the histidine imidazole group was hypothesized to be the major factor causing the elevation of the pK_as (Zhang, M., et al., 1994). Figure 1 shows stereoviews of the active site amino acid side chains of wild-type BPTP as well as the residues that were examined in detail in this study. The two side chain carboxylates closest to the His-72 imidazole nitrogens are Glu-23 (3.3 Å) and Asp-42 (4.3 Å). A 0.63 unit greater decrease was observed in the pK_a of His-72 in E23A as compared to D42A, presumably because Glu-23 is 1 Å closer than Asp-42 to His-72. A greater decrease in the His-72 pK_a was also calculated for E23A than for D42A. The greatest decrease in pK_a for His-72 was observed for the E23A/D42A mutant. Both of the stabilizing negative charges were no longer present, and a putative hydrogen bond from the imidazole ring to Glu-23 was absent, thus causing a dramatic decrease in the pK_a of His-72. The Glu-23 and Asp-42 carboxylate side chains are 15.7 and 20.6 Å from the His-66 imidazole nitrogens, respectively. As expected, the measured and calculated changes in pK_a of His-66 were negligible for mutants involving these residues.

The Glu-139 carboxylate is 3.6 Å from the imidazole nitrogens of His-66 and 21 Å from the His-72 imidazole nitrogens. When Glu-139 was replaced by a neutral alanine, a significant decrease in the pK_a of His-66 was both observed and calculated. No substantial change in the pK_a of His-72 was observed or calculated. The His-66 pK_a of E139A decreased by 1.24 units while the His-72 pK_a of D42A decreased by 1.69 units, although Glu-139 is 0.70 Å closer to His-66 than Asp-42 is to His-72. The difference in accessibility to solvent and consequent exposure of His-66 to a larger average dielectric may be one reason that its pK_a was not reduced as much as that of His-72 when a single carboxylate was removed. Other factors that could elevate the pK_a of the His-66 imidazole are the coplanar position of a nearby aromatic ring (Tyr-142, ∼4 Å) as well as its location at the C-terminus of an α-helix (Loewenthal et al., 1992; Sancho et al., 1992). The hydrogen bonding network inferred from the crystal structure is also more extensive for the active site region near His-72. Consequently, a single mutation of a carboxylate to a neutral residue near the His-72 imidazole side chain may cause a larger decrease in its pK_a compared to a similar single mutation near His-66, because a hydrogen bond as well as a negatively charged group is removed in the former case. The crystal structure of BPTP shows that His-66 is at the protein surface and His-72 is less exposed. The solvent accessibility and side chain

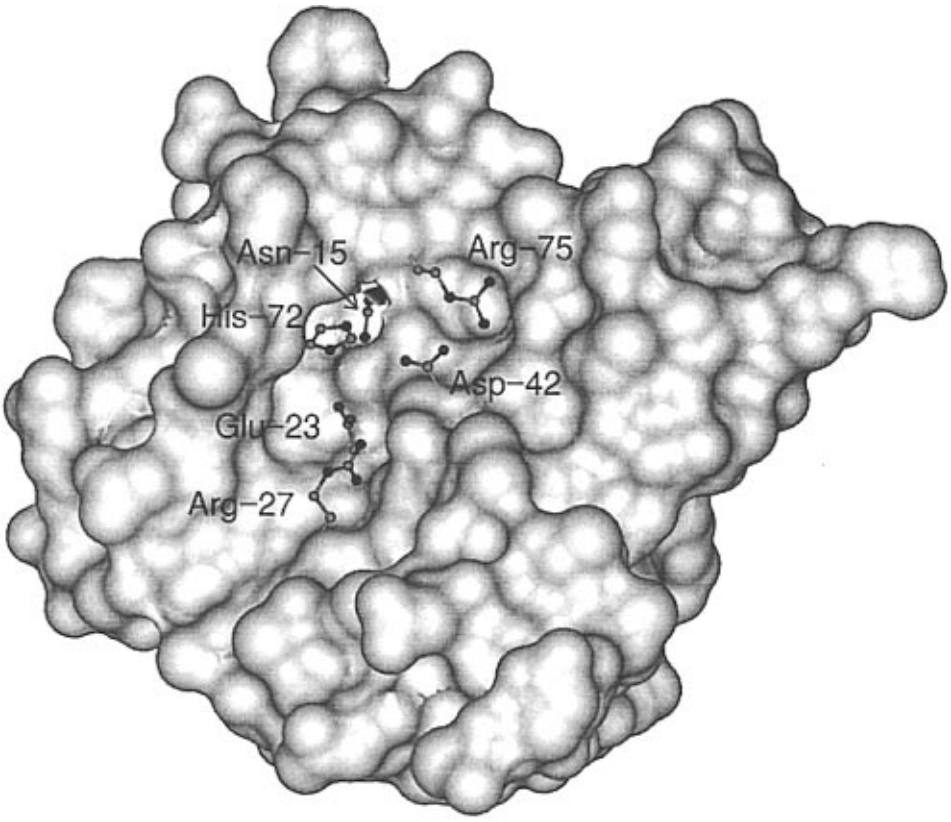

FIGURE 5: Connolly surface representation of wild-type BPTP showing the relative orientations and solvent accessibility of important charged side chains near His-72. The drawing was made using the X-ray crystal structure coordinates (Zhang et al., 1997) and Insight II version 95.0 (Biosym/MSI).

flexibility of His-72 are both substantially less than for His-66, which would result in greater susceptibility of His-72 to electrostatic changes within the protein. A histidine with greater solvent accessibility will have less ^{1}H NMR line broadening than a more buried histidine because the proton exchange rate is higher for the imidazole nitrogens, and the correlation time of a mobile side chain is usually much faster. The differences between His-66 and His-72 line widths that were observed in the ^{1}H NMR spectra for the proteins in this study indicated that the His-72 side chain was less mobile and less solvent-exposed than that of His-66, and that its mobility increased when nearby carboxylates were mutated to neutral alanines. This is consistent with the position of each histidine in the X-ray crystal structure.

The Q143E mutant was constructed to test whether introducing a second nearby negatively charged carboxylate group (~3.9 Å) would elevate the pK_a of His-66 to a value near that of His-72 in wild-type BPTP. The lack of any significant effect on the His-66 pK_a is probably due in part to the flexibility of the Glu-143 side chain. It is located at the protein surface, which allows the carboxylate group enough movement to be positioned away from the imidazole ring. This would be expected to substantially reduce the electrostatic interaction with the His-66 side chain. The exposure to solvent for both the His-66 imidazole and the Glu-143 carboxylate also places them in a higher dielectric environment which would dampen the electrostatic interaction between them.

The pK_a values of the histidine residues can be influenced by a number of factors, including the negatively charged groups studied by mutagenesis, positively charged groups, or the burial of the histidines away from solvent. In the current study, the effect of positively charged groups near each histidine was not examined by mutagenesis techniques because few positively charged residues appeared close enough to either histidine to have a significant effect. On the other hand, the effects of positive charges are present in the theoretical calculations through the $\Delta\Delta G_{back}$ term of eq 4 (since the Lys and Arg residues are regarded as fixed in their positively charge states). Arg-27 and Arg-75 are the only arginine or lysine residues less than 10 Å from His-72 (their distances are 6.1 and 7.7 Å, respectively). No arginine or lysine residues are within 10 Å of His-66.

The case of His-72 is of particular interest because of its interaction with a residue in the active site loop, and because it involves a number of large interactions (Zhang, M., et al., 1994; Evans et al., 1996). Figure 5 shows the disposition of charged side chains near His-72. His-72, Glu-23, and Arg-27 form a vertical chain of closely interacting residues from the top to the bottom in the figure, with Asp-42 and Arg-75 to the right. Arg-27 is 2.78 Å from Glu-23 while Arg-75 is 2.84 Å from Asp-42 in wild-type BPTP. His-72 is not well exposed to solvent, and lies in a shallow vertical cleft in the protein along with Glu-23 and Asp-42. Asn-15 is located behind His-72 and makes hydrogen bonds to it. This may help stabilize the active site loop, of which Asn-15 is a part. This structural environment leads to several large terms in the theoretical calculations for His-72. The unfavorable energetics of burying a positive charge away from solvent tend to lower the pK_a of His-72 through the $\Delta\Delta G_{Born}$ term; this effect is −3.84 pK units in the CHARMM-19 wild-type calculations. Its intrinsic pK is further depressed by the background interactions with nontitrating charges (−1.94 pK_a units and including all arginines and

lysines), but it is raised by the interactions with negatively charged titrating groups to produce the final pK_a value of 10.18. Of the charge−charge interactions, Glu-23 contributes +4.11 pK units, Asp-42 contributes +1.78, Arg-27 contributes −0.82, and Arg-75 contributes −0.90 unit. The presence of large terms of opposite sign obviously increases the difficulty of making accurate calculations for the wild-type pK_a value. These large interactions also provide an explanation for the excessively large ΔpK_a estimates calculated for the E23A mutant and suggest a structural explanation for the smaller shift seen experimentally. The calculated shift is mostly due to the loss of the +4.11 pK unit interaction with Glu-23, while the pK_a lowering effects of the interaction with Arg-27 and the $\Delta\Delta G_{Born}$ term continue to have values similar to those in the wild type. Examination of the structure shows that Arg-27 could be extended out into the solvent, away from His-72, and the loss of its salt bridge with Glu-23 in the mutant might allow this to occur. The truncation of the Glu-23 side chain slightly increases the solvent exposure of His-72, and it seems plausible that greater exposure could occur due to minor structural changes caused by the mutation. Both of these effects would tend to raise the pK_a of His-72 in compensation for the loss of the interaction with the negative charge. It has been noted previously that the assumption of structural rigidity implicit in the type of theoretical calculations presented here can lead to exaggeration of pK shifts because of the neglect of structural changes that may moderate the shifts (Antosiewicz et al., 1994; Bashford & Karplus, 1990; You & Bashford, 1995).

With the capability of site-directed mutagenesis, it is possible to systematically change many, perhaps even most, residues in a protein. Consequently, not only should it be possible to place various types of charged or aromatic residues near each histidine in BPTP, but it may also be possible to place histidines at new locations in the enzyme. Strategically placed residues should provide additional interesting information about the electrostatic environment within BPTP. This could potentially be a useful empirical means of producing an electrostatic map of the protein, provided the manipulation does not significantly alter the structural integrity of the enzyme. Understanding the electrostatic potential within and around a protein can be valuable in determining its function or predicting interactions with other molecules. These techniques would also be extremely useful in the further testing of theoretical electrostatic models of proteins. Protein engineering studies toward this goal have been done previously (Loewenthal et al., 1992, 1993). The present experiments demonstrate that reasonable estimates of pK_a perturbations can be calculated using current approaches. They also suggest that further improvements can be achieved as relevant force fields are further refined. A close interplay between theoretical approaches and experimental validation such as that embodied in the present work is a critical requirement for efficient progress in the area.

REFERENCES

Antosiewicz, J., McCammon, J. A., & Gilson, M. K. (1994) *J. Mol. Biol. 238*, 415−436.

Antosiewicz, J., McCammon, J. A., & Gilson, M. K. (1996) *Biochemistry 35*, 7819−7833.

Bashford, D., & Karplus, M. (1990) *Biochemistry 29*, 10219−10225.

Bashford, D., & Gerwert, K. (1992) *J Mol. Biol.* 224, 473−486.

Bashford, D., Case, D. A., Dalvit, C., Tennant, L., & Wright, P. E. (1993) *Biochemistry 32*, 8045−8056.

Beroza, P., Fredkin, D. R., Okamura, M. Y., & Feher, G. (1991) *Proc. Natl. Acad. Sci. U.S.A. 88*, 5804−5808.

Botelho, L. H., & Gurd, F. R. N. (1978) *Biochemistry 17*, 5188−5196.

Botelho, L. H., Friend, S. H., Matthew, J. B., Lehman, L. D., Hanania, G. I. H., & Gurd, F. R. N. (1978) *Biochemistry 17*, 5197−5205.

Brooks, B. R., Bruccoleri, R. E., Olafson, B. D., States, D. J., Swaminathan, S., & Karplus, M. (1983) *J. Comput. Chem. 4*, 187−217.

Brünger, A. T., & Karplus, M. (1988) *Proteins: Struct., Funct., Genet. 4*, 148−156.

Chiarugi, P., Cirri, P., Camici, G., Manao, G., Fiaschi, T., Raugei, G., Cappugi, G., & Ramponi, G. (1994) *Biochem. J. 298*, 427−433.

Davis, J. P., Zhou, M.-M., & Van Etten, R. L. (1994a) *J. Biol. Chem. 269*, 8734−8740.

Davis, J. P., Zhou, M.-M., & Van Etten, R. L. (1994b) *Biochemistry 33*, 1278−1286.

Evans, B., Tishmack, P. A., Pokalsky, C., Zhang, M., & Van Etten, R. L. (1996) *Biochemistry 35*, 13609−13617.

Gilson, M. K. (1995) *Curr. Opin. Struct. Biol. 5*, 216−223.

Glasoe, P. K., & Long, F. A. (1960) *J. Am. Chem. Soc. 64*, 188−190.

Honig, B., & Nicholls, A. (1995) *Science 268*, 1144−1149.

Kraulis, P. (1991) *J. Appl. Crystallogr. 24*, 946−950.

Lawrence, G. L., & Van Etten, R. L. (1981) *Arch. Biochem. Biophys. 206*, 122−131.

Levitt, M. H., Freeman, R., & Frenkiel, T. (1982) *J. Magn. Reson. 47*, 328−330.

Li, N. C., Tang, P., & Mathur, R. (1961) *J. Am. Chem. Soc. 65*, 1074−1076.

Li, Y., & Strohl, W. R. (1996) *J. Bacteriol. 178*, 136−142.

Linderstrøm-Lang, K. (1924) *C. R. Lab. Carlsberg 15(7)*, 1−29.

Loewenthal, R., Sancho, J., & Fersht, A. R. (1992) *J. Mol. Biol. 224*, 759−770.

Loewenthal, R., Sancho, J., Reinikainen, T., & Fersht, A. R. (1993) *J. Mol. Biol. 232*, 574−583.

Logan, T. M., Shou, M.-M., Nettesheim, D. G., Meadows, R. P., Van Etten, R. L., & Fesik, S. W. (1994) *Biochemistry 33*, 11087−11096.

MacKerell, A. D., Jr., Bashford, D., Bellott, M., Dunbrack, R. L., Jr., Field, M. J., Fischer, S., Gao, J., Guo, H., Ha, S., Joseph, D., Kuchnir, L., Kuczera, K., Lau, F. T. K., Mattos, C., Michnick, S., Ngo, T., Nguyen, D. T., Prodhom, P., Roux, B., Schlenkrich, M., Smith, J. C., Stote, R., Straub, J., Wiorkiewicz-Kuczera, J., & Karplus, M. (1992) *FASEB J. 6*, A143.

Markley, J. L. (1973) *Biochemistry 12*, 2245−2250.

Markley, J. L. (1975a) *Acc. Chem. Res. 8*, 70−80.

Markley, J. L. (1975b) *Biochemistry 14*, 3546−3554.

Markley, J. L. (1975c) *Biochemistry 14*, 3554−3561.

Markley, J. L., & Finkenstadt, W. R. (1975) *Biochemistry 14*, 3554−3561.

Matthew, J. B., & Gurd, F. R. N. (1986) *Methods Enzymol.* 130, 413−436.

Meadows, D. H. (1972) *Methods Enzymol 26*, 638−653.

Meadows, D. H., Markley, J. L., Cohen, J. S., Jardetsky, O. (1967) *Proc. Natl. Acad. Sci. U.S.A. 58*, 1307−1313.

Ostanin, K., Pokalsky, C., Wang, S., & Van Etten, R. L. (1995) *J. Biol. Chem. 270*, 18491−18499.

Ramette, R. W. (1981) *Chemical Equilibrium and Analysis*, p 361, Addison-Wesley Publishing Co., Reading, MA.

Ramponi, G. (1994) *Adv. Protein Phosphatases 8*, 1−25.

Reiher, W. E., III. (1985) Ph.D. Thesis, Harvard University.

Roberts, G. C. K., Meadows, D. H., & Jardetzky O. (1969) *Biochemistry 8*, 2053−2056.

Russell, A. J., Thomas, P. G., & Fersht, A. R. (1987) *J. Mol. Biol. 193*, 803−813.

Saini, M. S., Buchwald, S. L., Van Etten, R. L., & Knowles, J. R. (1981) *J. Biol. Chem. 256*, 10453−10455.

Sancho, J., Serrano, L., & Fersht, A. R. (1992) *Biochemistry 31*, 2253−2258.

Shimohama, S., Fujimoto, S., Taniguchi, T., & Kimura, J. (1994) *Brain Res. 662*, 185−188.
Shire, S. J., Hanania, G. I. H., & Gurd, R. N. (1974a) *Biochemistry 13*, 2967−2974.
Shire, S. J., Hanania, G. I. H., & Gurd, R. N. (1974b) *Biochemistry 13*, 2974−2979.
Su, X.-D., Taddei, N., Stefani, M., Ramponi, G., & Nordlund, P. (1994) *Nature 370*, 575−578.
Sudmeier, J. L., Evelhoch, J. L., &Jonsson, N. B.-H. (1980) *J. Magn. Reson. 40*, 377−390.
Tanford, C., & Kirkwood, J. G. (1957) *J. Am. Chem. Soc. 79*, 5333−5339.
Vandeyar, M. A., Weiner, M. P., Hutton, C. J., & Batt, C. A. (1988) *Gene 65*, 129−133.
Waheed, A., Laidler, P. M., Wo, Y.-Y. P., & Van Etten, R. L. (1988) *Biochemistry 27*, 4265−4273.
Warwicker, J., & Watson, H. C. (1982) *J. Mol. Biol. 157*, 671−679.
Wo, Y.-Y. P., Zhou, M.-M., Stevis, P., Davis, J. P., Zhang, Z.-Y., & Van Etten, R. L. (1992a) *Biochemistry 31*, 1712−1721.
Wo, Y.-Y. P., McCormack, A. L., Shabanowitz, J., Hunt, D. F., Davis, J. P., Mitchell, G. L., & Van Etten, R. L. (1992b) *J. Biol. Chem. 267*, 10856−10865.
Yang, Q., & Tonks, N. K. (1993) *Adv. Protein Phosphatases 7*, 359−372.
You, T., & Bashford, D. (1995) *Biophys. J. 69*, 1721−1733.
Zhang, M., Van Etten, R. L., & Stauffacher, R. L. (1994) *Biochemistry 33*, 11097−11105.
Zhang, M., Stauffacher, C. V., & Van Etten, R. L. (1995) *Adv. Protein Phosphatases 9*, 1−23.
Zhang, M., Zhou, M., Van Etten, R. L., & Stauffacher, C. V. (1997) *Biochemistry 36*, 15−23.
Zhang, Z.-Y., & Van Etten, R. L. (1990) *Arch. Biochem. Biophys. 282*, 39−49.
Zhang, Z.-Y., & Dixon, J. E. (1994) *Adv. Enzymol Relat.Areas Mol. Biol.68*, 1−36.
Zhang, Z., Harms, E., & Van Etten, R. L. (1994) *J. Biol. Chem. 269*, 25947−25950.
Zhou, M.-M., Davis, J. P., & Van Etten, R. L. (1993) *Biochemistry 32*, 8479−8486.

BI9712448